Application of the generalised radiance function for prediction of the mean RCS of bent chaotic ducts with apertures not normal to the duct axis .

Andrew Mackay

DERA Malvern, St Andrew's Road
Great Malvern, Worcs WR14 3PS, UK

Ref no: DERA/S&E/RAD/JP010585

March 2001

Abstract

A method is proposed to approximate the mean radar cross section (RCS) of a chaotic electrically large bent duct with an aperture not necessarily normal to the duct axis. This is based on a ray mapping of the generalised radiance function (GRF) associated with a random field. The field within the duct is assumed to be represented by a scalar function and a homogenous Schell model is assumed to describe the back-scattered transverse field at some cross section within the duct. The GRF associated with this field may then be mapped to a general aperture where the mean RCS can be determined. An analytic example is provided where a chaotic bent duct is terminated by a prism-shaped precursor structure.

1.1 Introduction

It has been shown that the ability to make accurate convergent predictions of general engine ducts at high frequency using conventional shooting-and-bouncing (SBR) ray based methods is curtailed by the effects of chaos [1, 2]. Random wave methods can be used to provide representative radar cross section (RCS) distributions for both straight and very bent chaotic ducts [3, 4] and the theory may be linked to the use of a Lambert form [5] for the mean RCS [4]. These methods assume a homogeneous aperture field distribution and an aperture which is approximately (locally) normal to the duct axis.

In this paper it is shown how the theory can be extended by local mapping of the duct fields. In much the same way as a ray transformation locally maps the electric (or magnetic) field between different regions of space, so a local ray mapping of a *generalised radiance function* [5] is proposed when the fields themselves are random (i.e. describable as a set of random waves). The theory is demonstrated under the assumption that the underlying field is a scalar one, though there is no reason why this should not be generalised to vector fields.

For scalar fields, the existence of a homogeneous Schell model allows the back-scattered field at a cross section within the duct (where the Schell model is valid) to be represented locally in terms of a generalised radiance function which expresses the local spatial and spectral distribution of radiated power. This distribution can be mapped to other places within the duct using a ray approach in the phase space of spatial (positional) and spectral (directional) dimensions. The RCS can then be computed as an integral over the transformed generalised radiance.

1.2 The generalised radiance and RCS

A generalised radiance function (GRF) is any function [5] which (loosely) describes an electromagnetic energy density, per unit solid angle per unit area, which quantifies the radiated power distribution in a particular direction from a particular source point in space. If the field on an aperture is describable by a homogeneous Schell model then the generalised radiance has all the features of an energy density, including the fact that it is a positive real quantity [5, section 5.7.2]. A common definition, employed here, assumes the form of a Wigner distribution in quantum mechanics. This is given by,

$$\mathcal{B}_\nu^{(0)}(\boldsymbol{\rho}, \boldsymbol{s}) = \left(\frac{k}{2\pi}\right)^2 \cos\xi \int_\infty W^{(0)}(\boldsymbol{\rho} - \boldsymbol{\rho}'/2, \boldsymbol{\rho} + \boldsymbol{\rho}'/2, \nu) e^{ik\boldsymbol{s}_\perp \cdot \boldsymbol{\rho}'} d^2\rho' \tag{1}$$

Here, $\boldsymbol{\rho}$ represents a position in space, $\boldsymbol{s}$ represents a unit direction vector, $\boldsymbol{s}_\perp$ represents the transverse component of $\boldsymbol{s}$ in the plane of the aperture, ν represents the frequency of the (generally non-monochromatic) field, k is the associated wavenumber $k = 2\pi\nu/C$ where C is the speed of light and ξ is the angle made between $\boldsymbol{s}$ and the normal to the aperture. The integration is performed over the plane of the aperture. $W^{(0)}(\boldsymbol{\rho}_1, \boldsymbol{\rho}_2, \nu)$ is the cross spectral density. Angles and vectors are defined such that,

$$\begin{array}{ll} \boldsymbol{\rho} = x\hat{\boldsymbol{x}} + y\hat{\boldsymbol{y}} & \boldsymbol{\rho}' = x'\hat{\boldsymbol{x}} + y'\hat{\boldsymbol{y}} \\ \boldsymbol{s} = \cos\xi\,\hat{\boldsymbol{z}} + \sin\xi\,\boldsymbol{s}_\perp & \boldsymbol{s}_\perp = \cos\phi\,\hat{\boldsymbol{x}} + \sin\phi\,\hat{\boldsymbol{y}} \end{array} \tag{2}$$

Under the homogeneous Schell model, the cross spectral density across an electrically large spatial section may be represented [5] by,

$$W^{(0)}(\boldsymbol{\rho}_1, \boldsymbol{\rho}_2, \nu) = [S^{(0)}(\boldsymbol{\rho}_1, \nu)]^{1/2}[S^{(0)}(\boldsymbol{\rho}_2, \nu)]^{1/2} g^{(0)}(\boldsymbol{\rho}_1 - \boldsymbol{\rho}_2, \nu) \tag{3}$$

where $S^{(0)}(\boldsymbol{\rho}, \nu)$ is the spectral density which is assumed constant over the aperture for electrically large apertures and $g^{(0)}(\boldsymbol{\rho}, \nu)$ is the spectral degree of coherence. Following [4], a monochromatic limit is assumed so that $\nu \to \omega_0/(2\pi)$ and $k \to k_0$, where k_0 is the free space wavenumber and ω_0 is the angular frequency with harmonic time dependence of the form $e^{i\omega_0 t}$. All ensemble statistics which are calculated with respect to time t over a non-zero bandwidth are assumed, in the zero bandwidth limit, to be equal to those based on an ensemble over small variations in duct geometry which are large compared to a wavelength in the high frequency (zero wavelength) limit [3, 4].

When $W^{(0)}$ takes the form (3) and provided $g^{(0)}(\boldsymbol{\rho}, \nu)$ decays fast enough as $|\boldsymbol{\rho}| \to \infty$ (true for bent ducts which satisfy a Lambert form [4]) then it can be shown [5, section 5.7.3] that,

$$\mathcal{B}_\nu^{(0)}(\boldsymbol{\rho}, \boldsymbol{s}) = k^2 S^{(0)}(\boldsymbol{\rho}, \nu) \tilde{g}^{(0)}(k\boldsymbol{s}_\perp, \nu) \cos\xi \tag{4}$$

where $\tilde{g}^{(0)}(k\boldsymbol{s}_\perp, \nu)$ is the Fourier transform of $g^{(0)}(\boldsymbol{\rho}, \nu)$. The radiant intensity, $J(\boldsymbol{s}, \nu)$, represents the power radiated per unit solid angle per frequency interval by an aperture orientated at angle ξ to the observation direction $\boldsymbol{s}$. This may be given [5] as a spatial integral over the GRF,

$$J(\boldsymbol{s}, \nu) = \cos\xi \int_A \mathcal{B}_\nu^{(0)}(\boldsymbol{\rho}, \boldsymbol{s}) d^2\rho \tag{5}$$

where A represents the domain of the aperture. In the monochromatic limit the radiant intensity at the duct aperture is proportional to the mean RCS as described in [4]. In this limit,

$$J(\boldsymbol{s}, \nu) = J_\delta(\boldsymbol{s}, \boldsymbol{s}_{in}) \delta(\nu - (\omega_0/2\pi)) \tag{6}$$

and the mean RCS is,

$$\overline{\sigma} = \frac{4\pi J_\delta(\boldsymbol{s}, \boldsymbol{s}_{in})}{P_0(\boldsymbol{s}_{in})} \tag{7}$$

where $P_0(\boldsymbol{s}_{in})$ is a positive function of the incidence direction, $\boldsymbol{s}_{in}$, of an incident plane wave. $P_0(\boldsymbol{s}_{in})$ represents the total scattered power per unit incident wave projected area. For a lossless duct with aperture very large compared to a wavelength,

$$P_0(\boldsymbol{s}_{in}) = \frac{1}{A_1(\boldsymbol{s}_{in}) \cos\xi_{in}} \int_0^{2\pi} d\phi \int_0^{\pi/2} J_\delta(\boldsymbol{s}, \boldsymbol{s}_{in}) \sin\xi \, d\xi \tag{8}$$

where A_1, possibly a function of $\boldsymbol{s}_{in}$, represents that part of the aperture for which the wave enters deep within the duct. For an aperture normal to the duct axis, $A_1 \approx A$. All angles subscripted by "*in*" represent angles of incidence defined as in (2).

1.3 Duct precursor sections and phase space mapping

Although the field transverse to the duct axis can be modelled in the manner described in [3, 4], these models are not directly applicable to arbitrary apertures. Firstly, a general aperture will allow the

reflection of a significant part of an incident wave in a coherent (non-random) manner. Secondly, a radiated field which is pseudo-random deep within the duct may perhaps only escape through a very selective range of angles. This constitutes a filtering operation which colours the distribution. To account for these effects we will consider a general duct and its aperture as a union of a *duct precursor* containing the aperture and a duct with opening transverse to the duct axis. This is illustrated in figure 1.

The duct precursor is taken to be of length such that the slanted aperture, B, intersects the duct cross section, A, at just one point on the duct surface. It is also assumed that if the precursor is absent, the previously considered cross spectral density models [3, 4] are valid; thus all rays entering the duct at A undergo a large number of randomising bounces before they return back through A. Two sets of surface-of-section phase space coordinates are considered, (ξ, ϕ, x, y) and (ξ', ϕ', x', y'). The first unprimed set is with respect to the duct cross section A; ξ is the angle made by a ray that intercepts A with respect to the z-axis (which is the duct axis at A), x, y are the transverse coordinates of the ray intercept on A and ϕ is the angle made between the projection of a ray at A with the x-axis. Similarly ξ' and ϕ' are the angles made at B with respect to the primed coordinates defined with respect to the unit vectors,

$$\begin{aligned} \hat{\boldsymbol{x}}' &= \hat{\boldsymbol{x}} \cos\theta_n - \hat{\boldsymbol{z}} \sin\theta_n \\ \hat{\boldsymbol{y}}' &= \hat{\boldsymbol{y}} \\ \hat{\boldsymbol{z}}' &= \hat{\boldsymbol{x}} \sin\theta_n + \hat{\boldsymbol{z}} \cos\theta_n \end{aligned} \tag{9}$$

with the normal to the aperture at B defined in the x, z plane at an angle θ_n to the z-axis. Since the precursor is straight, the mapping is partially separable; i.e. for each angle ξ relative to the precursor duct axis the angle ξ is preserved on each bounce in this region.

If a ray enters from B into A with coordinates $(\xi_{in}, \phi_{in}, x_{in}, y_{in})$, we assume that on exit from A (from the duct-proper) the coordinates $\phi_{out}, x_{out}, y_{out}$ may attain any permitted value of ϕ, x or y (i.e. $0 \leq \phi < 2\pi$, $(x, y) \in A$) with equal probability. It is also assumed that the phase delay introduced by the duct between entry and exit through A is a random function of ϕ_{in}, x_{in} or y_{in}. For sufficiently bent ducts the phase delay is random and is also a random function of ξ. It is not necessary (or generally possible) to compute a deterministic mapping of the electromagnetic fields between entry and exit coordinates on A in the high frequency limit. Instead, a mapping of the ray probability density is required. For a sufficiently large number of rays the probability density is simply proportional to the density of points on the surface of section in phase space.

It is necessary to determine the GRF on the aperture B in the primed coordinate system as a function of the GRF on A in the unprimed system taken in the absence of the precursor. The former is defined as $\mathcal{B}^{(0)}_{\nu,(BAB)}$ and the latter as $\mathcal{B}^{(0)}_{\nu,(A)}$. To determine the former it is necessary to consider all rays entering at B which impinge on A and which exit from A back to B.

Not all rays entering B will reach A, though all those entering from A will exit B since the duct precursor is assumed straight. Rays can be defined on a surface of section coordinated by x, y, ϕ and ξ on an aperture. The phase space section at B can be divided into two distinct regions $\mathcal{S}_{B1}$ and $\mathcal{S}_{B2}$, such that $\mathcal{S}_{B1} \cap \mathcal{S}_{B2} = 0$. The entire phase space section at A, $\mathcal{S}_A$, maps one-to-one with $\mathcal{S}_{B1}$. There is in general a non-zero RCS contribution from both $\mathcal{S}_{B1}$ and $\mathcal{S}_{B2}$, the latter representing the contribution of rays which are reflected before entering the duct-proper. Only the $\mathcal{S}_{B1}$ contribution will be considered in this paper since the specular contribution can be determined using conventional SBR or physical optics methods.

To determine RCS contributions from $\mathcal{S}_{B1}$, it is necessary to consider a density mapping in both directions from B to A and then back from A to B. The first represents the dependence on angle of incidence, the second with respect to scatter angle.

The power radiated at a frequency ν into an element of solid angle $d\Omega$ by an element of area $d\sigma$ is given [5, section 5.7.2] by,

$$d^2\mathcal{F}_\nu = \mathcal{B}^{(0)}_\nu(\boldsymbol{\rho}, \boldsymbol{s}) \cos\xi \, d\sigma d\Omega \tag{10}$$

Let $m_{BA}(\boldsymbol{\rho}', \boldsymbol{s}'; \boldsymbol{\rho}, \boldsymbol{s})$ be the mapping density between the generalised radiance from all coordinates $(\boldsymbol{\rho}, \boldsymbol{s})$ in A to the coordinate $(\boldsymbol{\rho}', \boldsymbol{s}')$ in B. This is the ratio of the density of points on the surface of section in the neighbourhood of $(\boldsymbol{\rho}', \boldsymbol{s}')$ in B to the density of points in the neighbourhood of $(\boldsymbol{\rho}, \boldsymbol{s})$ in A (such that any point in the neighbourhood of a point $(\boldsymbol{\rho}, \boldsymbol{s})$ in A maps to a point in the neighbourhood of $(\boldsymbol{\rho}', \boldsymbol{s}')$ in B).

Using conservation arguments it is possible to show that,

$$\begin{aligned}\cos\xi'_{in} \cos\xi' \, \mathcal{B}^{(0)}_{\nu,(BAB)}(\boldsymbol{\rho}', \boldsymbol{s}'; \boldsymbol{\rho}'_{in}, \boldsymbol{s}'_{in}) = m_{BA}(\boldsymbol{\rho}', \boldsymbol{s}'; \boldsymbol{\rho}_0, \boldsymbol{s}_0) m_{BA}(\boldsymbol{\rho}'_{in}, \boldsymbol{s}'_{in}; \boldsymbol{\rho}_{in,0}, \boldsymbol{s}_{in,0}) \\ \times \cos\xi_0 \cos\xi_{in,0} \, \mathcal{B}^{(0)}_{\nu,(A)}(\boldsymbol{\rho}_{in,0}, \boldsymbol{s}_{in,0}; \boldsymbol{\rho}_0, \boldsymbol{s}_0)\end{aligned} \tag{11}$$

where the "$in, 0$" subscript refers to the coordinates of a ray incident on A from B and the single "0" subscript refers to the coordinates of a ray emitted from A, returning from the duct-proper. This is the general relationship between the GRF on the slanted aperture given the GRF on the duct cross section, under the assumption that the ray model well describes the precursor section. Under the ray representation, m_{BA} is the ratio of the area in the phase space surface of section in the neighbourhood of a single point in A to that of B. This is the magnitude of the Jacobian of the transformation between the surfaces of section at A and B,

$$m_{BA}(\boldsymbol{\rho}', \boldsymbol{s}'; \boldsymbol{\rho}, \boldsymbol{s}) = \left| \frac{\partial(\boldsymbol{\rho}, \boldsymbol{s})}{\partial(\boldsymbol{\rho}', \boldsymbol{s}')} \right| \tag{12}$$

This is computable using ray tracing provided the number of ray bounces and Lyapunov exponent of the compound deviation matrix [1, 2] is not too large between A and B; i.e. provided a convergent ray tracing is possible between A and B, with insufficient space for the development of chaos in this region. From (5), the radiant intensity from the phase space contribution $\mathcal{S}_{B1}$ at the slanted aperture

is given by,

$$J_{B1,\rho}(\boldsymbol{s}', \boldsymbol{\rho}'_{in}, \boldsymbol{s}'_{in}; \nu) = \cos\xi' \iint_{B\cap\mathcal{S}_{B1}} \mathcal{B}^{(0)}_{\nu,(BAB)}(\boldsymbol{\rho}', \boldsymbol{s}'; \boldsymbol{\rho}'_{in}, \boldsymbol{s}'_{in}) d^2\rho' \tag{13}$$

This describes the scattered intensity given a single incident ray with unit power defined by the coordinates $(\boldsymbol{\rho}'_{in}, \boldsymbol{s}'_{in})$. The integration is over that region of the aperture B for which scattered rays exist, i.e. the intersection of B with the phase space set $\mathcal{S}_{B1}$. For an incident plane wave in the direction $\boldsymbol{s}'_{in}$, the radiant intensity is an integration of $J_{B1,\rho}$ over the normalised spectrum of rays required to synthesise the incident wave. Under the standard definition (i.e. using the shooting-and-bouncing interpretation) this is a simple integration over $\boldsymbol{\rho}'_{in}$. If the incident wave has unit intensity, then each contributing ray has the same direction with intensity $\cos\xi'_{in}/A_B$, where A_B is the area of the aperture B. Thus the $\mathcal{S}_{B1}$ contribution to the radiant intensity generated by an incident plane wave is given by,

$$J_{B1}(\boldsymbol{s}', \boldsymbol{s}'_{in}; \nu) = \frac{\cos\xi'_{in}\cos\xi'}{A_B} \iint_{B\cap\mathcal{S}_{B1}} d^2\rho' \iint_{B\cap\mathcal{S}_{B1}} d^2\rho'_{in}\ \mathcal{B}^{(0)}_{\nu,(BAB)}(\boldsymbol{\rho}', \boldsymbol{s}'; \boldsymbol{\rho}'_{in}, \boldsymbol{s}'_{in}) \tag{14}$$

In the monochromatic limit, replace $J_{B1}(\boldsymbol{s}', \boldsymbol{s}'_{in}; \nu) \to J_{B1,\delta}(\boldsymbol{s}', \boldsymbol{s}'_{in})$ with $\nu = \omega_0/2\pi$ and $k = k_0$. The mean RCS contribution from those rays which enter the duct-proper may then be written, using (7), as,

$$\overline{\sigma}_{\mathcal{S}_{B1}} = \frac{4\pi J_{B1,\delta}(\boldsymbol{s}', \boldsymbol{s}'_{in})}{P_0(\boldsymbol{s}'_{in})} \tag{15}$$

The total mean RCS can simply be expressed as the sum of contributions,

$$\overline{\sigma} = \overline{\sigma}_{\mathcal{S}_{B1}} + \overline{\sigma}_{\mathcal{S}_{B2}} \tag{16}$$

where $\overline{\sigma}_{\mathcal{S}_{B2}}$ is the coherent contribution from rays which are reflected from the precursor structure before reaching the aperture of the duct-proper, A.

1.4 Example of a prism shaped precursor

This example considers a long bent chaotic duct which slowly tapers into a rectangular cross section, with a rectangular aperture cut slant-wise into the duct as illustrated in figure 2. It is possible to show that for a sufficiently bent duct obeying a homogeneous Schell model [5, 4],

$$\tilde{g}^{(0)}(k_0\boldsymbol{s}_\perp, \omega_0/2\pi) = \frac{1}{2\pi k_0^2 \cos\xi} \tag{17}$$

and hence using (4),

$$\mathcal{B}^{(0)}_{\nu,(A)} = B_0 \tag{18}$$

where B_0 is a constant, independent of $\boldsymbol{\rho}_{in}$, $\boldsymbol{s}_{in}$, $\boldsymbol{\rho}$ or $\boldsymbol{s}$.

The rectangular cross section taper has dimensions L_x by L_y in the x and y directions, respectively. Geometric projections of this structure looking onto the prism from above (y-z plane) and to the side (x-z plane) are illustrated in figure 2 and designated by the labels "$\perp$" and "$\parallel$", respectively. The ray

projection angles θ, η and θ', as illustrated in the figure, are defined by

$$\cos\theta = \frac{\cos\xi}{\sqrt{\sin^2\xi\cos^2\phi + \cos^2\xi}} \tag{19}$$

$$\cos\eta = \frac{\cos\xi}{\sqrt{\sin^2\xi\sin^2\phi + \cos^2\xi}} \tag{20}$$

and

$$\cos\theta' = \frac{\cos\xi'}{\sqrt{\sin^2\xi'\cos^2\phi' + \cos^2\xi'}} \tag{21}$$

The ray density mapping $m_{BA}(\boldsymbol{\rho}', \boldsymbol{s}'; \boldsymbol{\rho}, \boldsymbol{s})$, is separable in the two projections;

$$m_{BA}(\boldsymbol{\rho}', \boldsymbol{s}'; \boldsymbol{\rho}, \boldsymbol{s}) = m_{BA}^{(\parallel)}(x', \theta'; x, \theta) m_{BA}^{(\perp)}(y', \eta'; y, \eta) \tag{22}$$

where $y' = y$ and $\eta' = \pm\eta$, with the + sign if the projected ray is reflected an even number of times (including the case where there is no reflection) and a $-$ sign if it is reflected an odd number of times before exiting through B.

Since $\mathcal{B}_{\nu,(A)}$ is assumed to be independent of spatial coordinates then the ray density mapping may be constructed from families of parallel rays delineated by the aperture boundary. Furthermore, it is also assumed that $\mathcal{B}_{\nu,(A)}$ is independent of ϕ or ϕ_{in} so that $\mathcal{B}_{\nu,(A)}$ is independent of the sign of ξ or ξ_{in}. First consider the $(\perp)$ projection. Here, the superposition of ray bundles in the + and $-\xi$ (and hence + and $-\eta$) directions gives rise to a constant unit ray density. The term $\cos\xi_{in,0}$ is also independent of y so the perpendicular density may be ignored and,

$$\cos\xi'_{in}\cos\xi'\,\mathcal{B}^{(0)}_{\nu,(BAB)}(\boldsymbol{\rho}', \boldsymbol{s}'; \boldsymbol{\rho}'_{in}, \boldsymbol{s}'_{in}) = m_{BA}^{(\parallel)}(\theta', x'; \theta_0, x_0) m_{BA}^{(\parallel)}(\theta'_{in}, x'_{in}; \theta_{in,0}, x_{in,0})$$

$$\times \cos\xi_0\cos\xi_{in,0}\,\mathcal{B}^{(0)}_{\nu,(A)}(\boldsymbol{\rho}_{in,0}, \boldsymbol{s}_{in,0}; \boldsymbol{\rho}_0, \boldsymbol{s}_0) \tag{23}$$

where θ_0 and x_0 refer to the ray coordinates on the $z = 0$ intercept arriving from aperture A and giving rise to a ray with coordinates θ' and x' on the $z' = 0$ intercept (aperture B). Similarly, $\theta_{in,0}$ and $x_{in,0}$ refer to the ray coordinates on the $z = 0$ intercept from an incident ray at B with coordinates θ'_{in} and x'_{in}.

In the Lambert model for which $\mathcal{B}^{(0)}_{\nu,(A)} = B_0$, the expression for J_{B1} in (14) separates and an independent integration of the $m_{BA}^{(\parallel)}$ terms is possible, involving scatter and incident angles with respect to $d^2\rho'$ and $d^2\rho$. A short examination shows that $\theta_{in,0} = \pm(\theta_n - \theta'_{in})$ and is also independent of x' in B for those rays which enter the duct-proper. Thus $\cos\xi_{in,0}$ is constant and can be taken outside the integral so,

$$J_{B1,\delta}(\boldsymbol{s}', \boldsymbol{s}'_{in}) = \frac{B_0 L_y^2 \cos\xi_0\cos\xi_{in,0}}{A_B} b(\boldsymbol{s}'_{in}) b(\boldsymbol{s}') \tag{24}$$

where

$$A_B = \frac{L_x L_y}{\cos\theta_n} \tag{25}$$

and

$$b(\boldsymbol{s}') = \int_{X'\cap\mathcal{S}_{B1}} m_{BA}^{(\parallel)}(\theta', x')dx' \tag{26}$$

The integration cover $X' \cap \mathcal{S}_{B1}(\boldsymbol{s}')$ refers to those x', for a given $\boldsymbol{s}'$, for which rays enter into the duct-proper. In order to determine $m_{BA}^{(\|)}$, a graphical representation of the parallel ray families is helpful, as illustrated in figure 3. Here, figures (a) to (g) represent stages as the incidence projection angle θ is decreased. Initially all rays are reflected (in this projection) exactly once (figures (a) to (c)). There is then a span (figures (d) to (e)) where some rays are reflected and some are not reflected. Finally (figures (f) to (g)) no rays are reflected.

Let $w(\theta')$ be the width of the ray family on the x' axis, as illustrated in the figure. Thus,

$$\begin{aligned} \theta' &= \theta_n - \theta \\ w(\theta') &= L_x \cos\theta / \cos\theta' \end{aligned} \tag{27}$$

Since $|\partial\theta'/\partial\theta| = 1$, $m_{BA}^{(\|)}(\theta', x') \equiv m_{BA}^{(\|)}(\theta', x'; \theta_0, x_0)$ may be identified as the ratio of the spatial ray density on B to that on A. This is just the ratio of the ray bundle width on A to the ray bundle width on B. There are 4 cases within $\mathcal{S}_{B1}$;

case 1: (see figs (a) to (c))

$$\begin{gathered} \text{for } 2w(\theta') < L_x/\cos\theta_n, \text{ i.e. } \theta_n - \pi/2 < \theta' < 2\theta_n - \pi/2 \\ m_{BA}^{(\|)}(\theta', x') = \begin{cases} \dfrac{\cos\theta'}{\cos(\theta' - \theta_n)} & \text{for } 2w(\theta') > x' > w(\theta') \\ \text{see } \textbf{case 4} & \text{otherwise} \end{cases} \end{gathered} \tag{28}$$

case 2: (see figs (d) to (e))

$$\begin{gathered} \text{for } \theta_n > \theta' > 2\theta_n - \pi/2 \\ m_{BA}^{(\|)}(\theta', x') = \begin{cases} \dfrac{\cos\theta' \sin\theta_n \tan(\theta_n - \theta')}{\cos\theta' - \cos\theta_n \cos(\theta_n - \theta')} & \text{for } L_x/\cos\theta_n > x' > w(\theta') \\ \text{see } \textbf{case 4} & \text{otherwise} \end{cases} \end{gathered} \tag{29}$$

case 3: (see figs (d) to (e))

$$\begin{gathered} \text{for } \pi/2 > \theta' > \theta_n \\ m_{BA}^{(\|)}(\theta', x') = \frac{\cos\theta'}{\cos(\theta' - \theta_n)} \end{gathered} \tag{30}$$

case 4: (see figs (f) and (g))

$$\begin{gathered} \text{for } \theta' < \theta_n \text{ AND } x' < w(\theta') \\ m_{BA}^{(\|)}(\theta', x') = \frac{\cos\theta'}{\cos(\theta' - \theta_n)} \end{gathered} \tag{31}$$

Note that $m_{BA}^{(\|)}(\theta', x')$ is always a piece-wise constant function of x' for geometries where the reflection boundaries are flat. The expression (26) for $b(\boldsymbol{s}')$ can now be evaluated over the three angular ranges described in cases (1) to (3) above. In fact, the latter two take the same form and,

$$b(\boldsymbol{s}') = \begin{cases} 2L_x & \text{for } \theta_n - \pi/2 < \theta' < 2\theta_n - \pi/2 \\ L_x \left(\dfrac{\cos\theta'}{\cos\theta_n \cos(\theta' - \theta_n)} \right) & \text{for } \pi/2 > \theta' > 2\theta_n - \pi/2. \end{cases} \tag{32}$$

The non-coherent contribution to the RCS, given by (15), may now be written as

$$\overline{\sigma}_{\mathcal{S}_{B1}} = \frac{4\pi}{L_x I_b} \cos\xi_0(\boldsymbol{s}')\, b(\boldsymbol{s}') \cos\xi'_{in}\, A_{B1}(\xi'_{in}, \phi'_{in}) \tag{33}$$

where I_b is defined by,

$$I_b = \frac{1}{L_x} \int_0^{2\pi} d\phi' \int_0^{\pi/2} \sin\xi' \cos\xi_0(\boldsymbol{s}') b(\boldsymbol{s}') d\xi' \tag{34}$$

Here, $\xi_0(\boldsymbol{s}')$ is the angle made by a ray emitted on the aperture A that gives rise to a ray in the direction $\boldsymbol{s}'$ at B. There are two possibilities in the x-z projection; either a ray is reflected or it is not. In both cases, using mirror symmetry,

$$\cos\xi_0(\boldsymbol{s}') = \cos\theta_n \cos\xi' + \sin\theta_n \sin\xi' \cos\phi' \tag{35}$$

and it is possible to show that $I_b = \pi$.

The term $A_{B1}(\xi'_{in}, \phi'_{in}) \equiv A_{B1}(\theta'_{in})$ is independent of η'_{in} and represents the area of aperture for which rays enter the duct-proper. Referring to figure 3, it may be observed that over the range $\pi/2 > \theta'_{in} > 2\theta_n - \pi/2$ all entry rays enter the duct-proper. For $\theta_n - \pi/2 < \theta'_{in} < 2\theta_n - \pi/2$, only those rays for which $x' < 2w(\theta'_{in})$ enter the duct. Thus,

$$A_{B1}(\theta'_{in}) = \begin{cases} 2L_x L_y \dfrac{\cos(\theta_n - \theta'_{in})}{\cos\theta'_{in}} & \text{for } \theta_n - \pi/2 < \theta'_{in} < 2\theta_n - \pi/2 \\ L_x L_y / \cos\theta_n & \text{for } \pi/2 > \theta'_{in} > 2\theta_n - \pi/2 \\ 0 & \text{otherwise} \end{cases} \tag{36}$$

The mean RCS may now be written in the form,

$$\overline{\sigma}_{\mathcal{S}_{B1}}(\boldsymbol{s}', \boldsymbol{s}'_{in}) = \frac{4\pi L_x L_y}{I_b} Q(\boldsymbol{s}') Q_{in}(\boldsymbol{s}'_{in}) \tag{37}$$

where Q and Q_{in} are respectively independent of $\boldsymbol{s}'_{in}$ and $\boldsymbol{s}'$. Using the geometrical relations,

$$\cos\xi'_{(in)} = \frac{\cos\theta'_{(in)} \cos\eta'_{(in)}}{\sqrt{1 - \sin^2\theta'_{(in)} \sin^2\eta'_{(in)}}} \tag{38}$$

and

$$\sin\xi'_{(in)} \cos\phi'_{(in)} = \cos\xi'_{(in)} \tan\theta'_{(in)} \tag{39}$$

where the subscript "(in)" may be absent or may refer to the subscript "in". It is straight forward to show that,

$$Q(\boldsymbol{s}') = \begin{cases} Q^{(1)}(\boldsymbol{s}') = \dfrac{2\cos\eta' \cos(\theta_n - \theta')}{\sqrt{1 - \sin^2\theta' \sin^2\eta'}} & \text{for } \theta_n - \pi/2 < \theta' < 2\theta_n - \pi/2 \\ Q^{(2)}(\boldsymbol{s}') = \dfrac{\cos\eta' \cos\theta'}{\cos\theta_n \sqrt{1 - \sin^2\theta' \sin^2\eta'}} & \text{for } 2\theta_n - \pi/2 < \theta' < \pi/2 \end{cases} \tag{40}$$

and, exactly of the same form,

$$Q_{in}(\boldsymbol{s}'_{in}) = \begin{cases} Q^{(1)}_{in}(\boldsymbol{s}'_{in}) = \dfrac{2\cos\eta'_{in} \cos(\theta_n - \theta'_{in})}{\sqrt{1 - \sin^2\theta'_{in} \sin^2\eta'_{in}}} & \text{for } \theta_n - \pi/2 < \theta'_{in} < 2\theta_n - \pi/2 \\ Q^{(2)}_{in}(\boldsymbol{s}'_{in}) = \dfrac{\cos\eta'_{in} \cos\theta'_{in}}{\cos\theta_n \sqrt{1 - \sin^2\theta'_{in} \sin^2\eta'_{in}}} & \text{for } 2\theta_n - \pi/2 < \theta'_{in} < \pi/2 \end{cases} \tag{41}$$

Thus, depending on the regions for θ' and θ'_{in},

$$\begin{aligned} Q^{(1)}(\boldsymbol{s}')Q^{(1)}_{in}(\boldsymbol{s}'_{in}) &= Q^{(1)}(\boldsymbol{s}'_{in})Q^{(1)}_{in}(\boldsymbol{s}') \\ Q^{(2)}(\boldsymbol{s}')Q^{(2)}_{in}(\boldsymbol{s}'_{in}) &= Q^{(2)}(\boldsymbol{s}'_{in})Q^{(2)}_{in}(\boldsymbol{s}') \\ Q^{(1)}(\boldsymbol{s}')Q^{(2)}_{in}(\boldsymbol{s}'_{in}) &= Q^{(2)}(\boldsymbol{s}'_{in})Q^{(1)}_{in}(\boldsymbol{s}') \end{aligned} \tag{42}$$

This demonstrates that the non-coherent mean RCS contribution is reciprocal over all angles, i.e. $\overline{\sigma}_{\mathcal{S}_{B1}}(\boldsymbol{s}', \boldsymbol{s}'_{in}) = \overline{\sigma}_{\mathcal{S}_{B1}}(\boldsymbol{s}'_{in}, \boldsymbol{s}')$. As an example, consider a prism geometry with $\theta_n = 50^o$, $L_x = L_y = 1$ m. Figure 4 shows the mean non-coherent contribution to the RCS, $\overline{\sigma}_{\mathcal{S}_{B1}}$, plotted on a dB scale as a function of $\theta' = \theta'_{in}$ for monostatic scattering. This is illustrated for values of $\eta' = \eta'_{in} = 0^o$, 30^o and 60^o. The RCS is a maximum when $\theta' = 2\theta_n - \pi/2$, which in this example occurrs at 10^o, when all rays incident on the aperture enter into the duct both with and without reflection (figure 3c).

1.5 Conclusions

It is demonstrated how the mean RCS, assuming a scalar field, can be computed from an integral over a GRF. The GRF over a general aperture can be determined by a suitable ray mapping of a GRF of given form elsewhere within the duct. This is particularly simple given a Lambert model [4] for the field at a plane perpendicular to the duct axis away from the aperture. An example is provided of a duct with a rectangular taper with an aperture taken as a section through the taper. A simple formula is then determined for the mean non-specular contribution to the RCS.

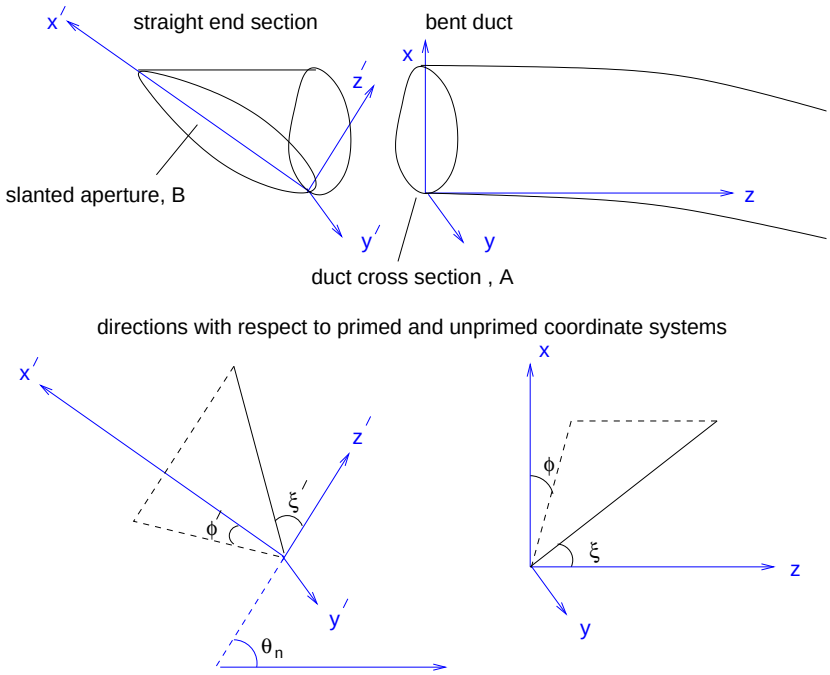

Figure 1. *A representation of a slanted aperture at the end of a bent duct.*

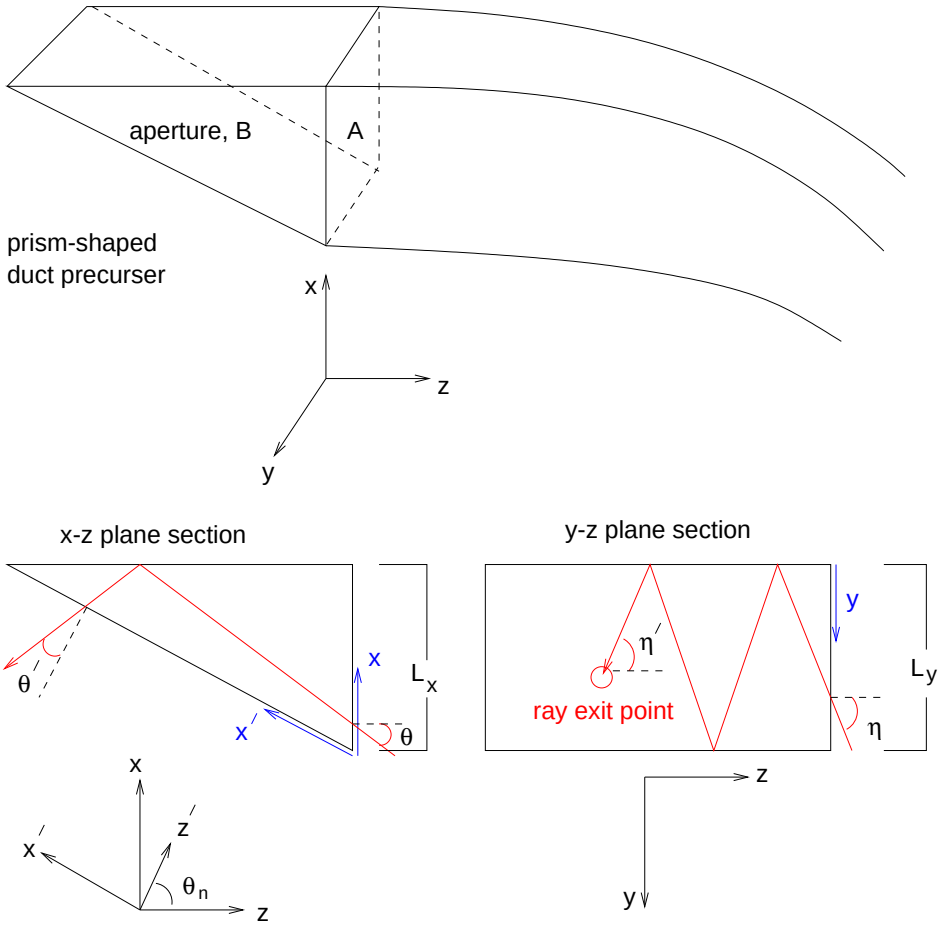

Figure 2. *Rectangular prism shaped duct precursor*

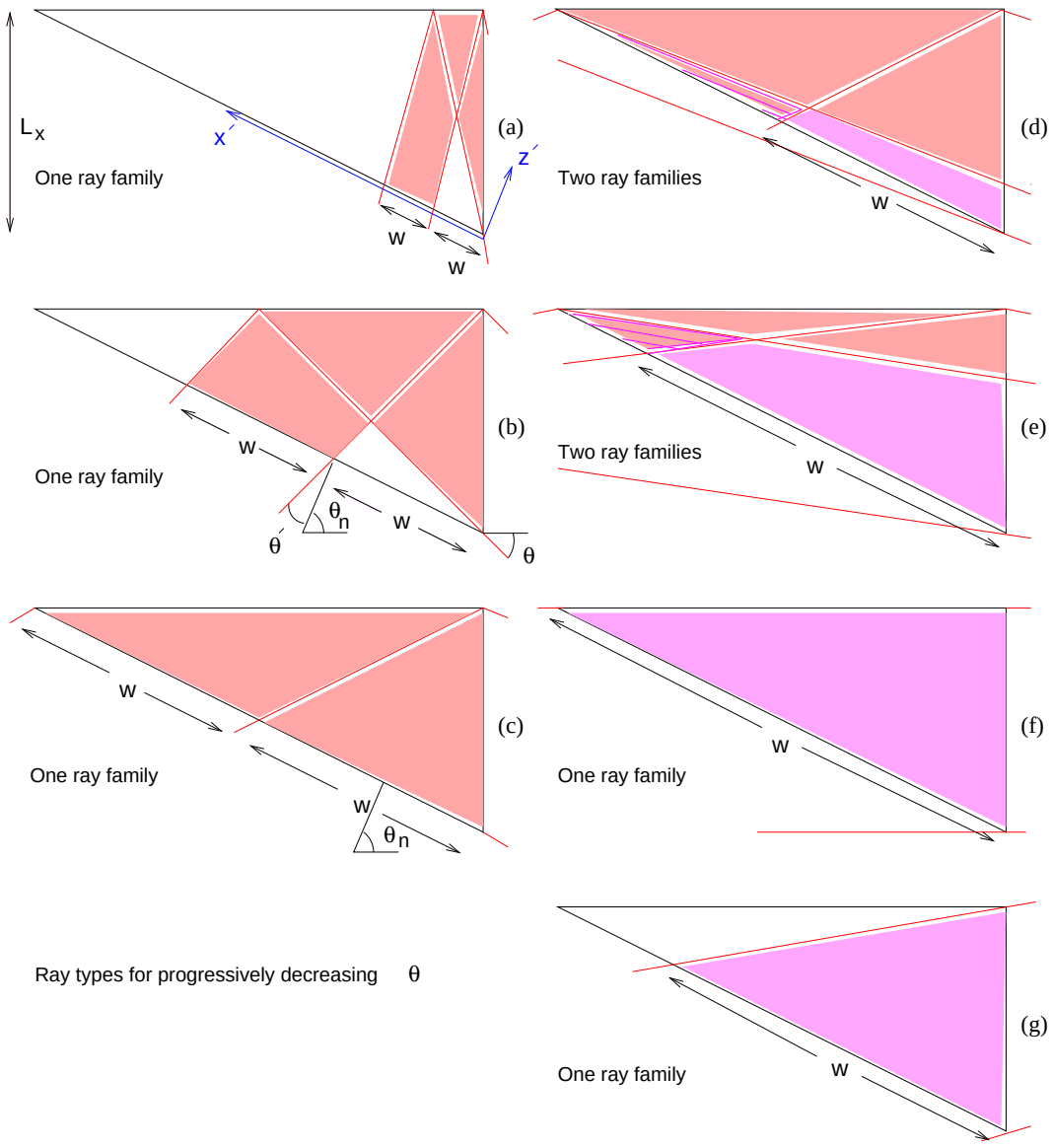

Figure 3. *Ray tracing in the parallel (x-z plane) projection.*

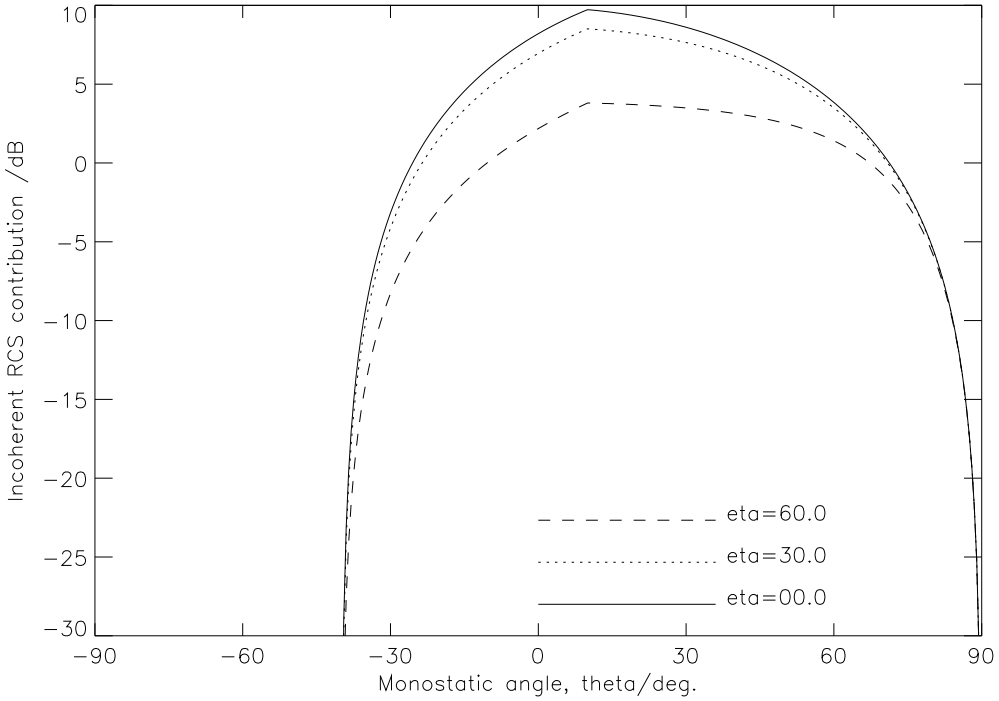

Figure 4. *Mean "non-coherent" contribution to the RCS from a prism-ended chaotic duct.*

References

[1] A.J.MACKAY *'Chaos theory and first order ray tracing in ducts'*, IEE Electronics Letters, Vol 34, No. 14, pp1388-1389, July 1998.

[2] A.J.MACKAY *'Application of chaos theory to ray tracing in ducts'*, IEE Proceedings Radar Sonar and Navigation, vol 146, No. 6, pp298-304, December 1999.

[3] A.J.MACKAY *'Random wave methods for the prediction of the RCS of homogeneous chaotic straight ducts'*, submitted to IEE Proceedings Radar Sonar and Navigation, 2001.

[4] A.J.MACKAY, *A random wave and Schell model for the mean RCS of bent chaotic ducts with a homogeneous scattered aperture field distribution*, submitted to IEE Proceedings Radar Sonar and Navigation, 2001.

[5] L.MANDEL, E.WOLF, *Optical coherence and quantum optics*, Cambridge University Press, 1995.